The role of cation diffusion facilitator CDF-1 in lipid metabolism in *Caenorhabditis elegans*

Ying Hu,[1,†] Yanli Wang,[2,†] Xuanjun Wang,[1] Xiaoyun Wu,[1] Lin Fu,[2] Xiayu Liu,[2] Yu Wen,[2] Jun Sheng,[1,*] and Jingjing Zhang [ID] [2,*]

[1]College of Food Science and Technology, Yunnan Agricultural University, Kunming 650201, China
[2]Center for Life Sciences, School of Life Sciences, Yunnan University, Kunming, Yunnan 650091, China

*Corresponding author: Yunnan University South Section, Chenggong Campus, East Outer Ring Road, Chenggong District, Kunming, Yunnan Province 650091, China. Email: zhangjingjing@ynu.edu.cn (J.Z.); shengjunpuer@163.com (J.S.)
[†]These authors contributed equally to this work.

Abstract

Zinc is one of the most important trace elements as it plays a vital role in many biological processes. As well, aberrant zinc metabolism has been implicated in lipid-related metabolic diseases. Previously, we showed that zinc antagonizes iron to regulate sterol regulatory element-binding proteins and the stearoyl-CoA desaturase (SREBP-SCD) pathway in lipid metabolism in the model organism *Caenorhabditis elegans*. In this study, we present the identification of another cation diffusion facilitator, CDF-1, which regulates lipid metabolism along with SUR-7 in response to zinc. Inactivation of SBP-1, the only homolog of SREBPs, leads to an increased zinc level but decreased lipid accumulation. However, either the *cdf-1(n2527)* or *sur-7(tm6523)* mutation could successfully restore the altered fatty acid profile, fat content, and zinc level of the *sbp-1(ep79)* mutant. Furthermore, we found that CDF-1/SUR-7 may functionally bypass SBP-1 to directly affect the conversion activity of SCD in the biosynthesis of unsaturated fatty acids and lipid accumulation. Collectively, these results consistently support the link between zinc homeostasis and lipid metabolism via the SREBP-SCD axis by the cation diffusion facilitators CDF-1 and SUR-7.

Keywords: zinc; sterol regulatory element-binding protein (SREBP); stearoyl-CoA desaturase (SCD); cation diffusion facilitator (CDF); lipid accumulation

Introduction

Zinc is one of essential trace elements for living organisms, and it plays numerous biological roles. For example, zinc determines both the structure and functionality of a variety of proteins, such as the metalloproteins. It can regulate both enzymatic activity and the stability of the proteins as either an activator or an inhibitor ion, and it modulates cellular signal transduction processes that are usually regulated by zinc transport or other interrelated proteins (Fukada *et al.* 2011; Chasapis *et al.* 2012; Escobedo-Monge *et al.* 2019). Thus, it is critical to maintain proper zinc homeostasis for living organisms.

Dysregulation of zinc homeostasis is related to many human diseases. In particular, deficiency of zinc has been shown to be closely associated with an altered lipid profile resulting in a series of lipid metabolism diseases, including obesity and comorbid conditions such as insulin resistance, type 2 diabetes, and inflammation (Costarelli *et al.* 2010; Błażewicz *et al.* 2013; Miao *et al.* 2013). Erythrocyte zinc levels are associated with body mass index and waist circumference (Błażewicz *et al.* 2013), and low zinc concentration was found in erythrocytes in obese women (Ennes Dourado Ferro *et al.* 2011). Moreover, there is a significant decrease in blood zinc levels in morbidly obese patients (de Luis *et al.* 2013). As well, zinc deficiency increases leptin production and exacerbates macrophage infiltration into adipose tissue in obese mice (Liu *et al.* 2013).

Zinc can be used as a nutrient to treat metabolic diseases. Zinc stimulates insulin secretion and increases the sensitivity to insulin. Therefore, zinc supplementation could improve insulin resistance, resulting in the improvement of blood pressure, glucose, and Low density lipoprotein (LDL) cholesterol serum level in obesity (Cruz *et al.* 2017; Olechnowicz *et al.* 2018). Obesity-related cardiac hypertrophy was exacerbated by zinc deficiency (ZD) in High fat diet/zinc deficiency (HFD/ZD) mice (de Luis *et al.* 2013), and this was attenuated by a zinc-supplemented diet (Wang *et al.* 2016). However, there may be deleterious effects with excessive zinc supplementation, since excessive zinc intake may cause an undesirable increase in HbA1c levels and high blood pressure (Miao *et al.* 2013). Again, the balance of zinc homeostasis in metabolism is critically important.

Maintenance of intracellular zinc homeostasis depends on the balance of zinc absorption, distribution, and excretion, which is mainly regulated by two protein families: metallothioneins and zinc transport proteins (Kimura and Kambe 2016). Zinc transport proteins are mainly responsible for mediating the compartmentalization of zinc into various organelles and vesicles for their storage, supplying zinc to various proteins that require it for functionality (Fukunaka and Fujitani 2018). Zinc transport proteins are divided into two major families: the zinc transporters or cation diffusion facilitator (ZnTs/CDFs) or solute-linked carrier family 30 (SLC30A), and the Zip (Zrt- and Irt-like proteins) family

or solute carrier family 39 A (SLC39A) (Liuzzi and Cousins 2004; Baltaci and Yuce 2018; Cotrim *et al.* 2019; Thokala *et al.* 2019). Several studies have shown that the expression of ZnT genes and disturbed zinc metabolism are associated with obesity and diabetes (Quraishi *et al.* 2005; Noh *et al.* 2014; Morais *et al.* 2019). The polymorphisms (SNPs) of ZnT8 have been connected with type 1 (Xu *et al.* 2011; Wenzlau and Hutton 2013) and type 2 diabetes (Rutter and Chimienti 2015; Drake *et al.* 2017; Virgili *et al.* 2018). ZnT5 is also involved in metabolic diseases (Cuadrado *et al.* 2018). However, the underlying mechanisms relating these ZnTs to metabolic diseases are largely unknown.

Our previous work showed that SUR-7, one of the zinc transport proteins in the model organism *Caenorhabditis elegans* (Yoder *et al.* 2004; Roh *et al.* 2013) synergistically affects zinc homeostasis and lipid metabolism via the sterol regulatory element-binding proteins and the stearoyl-CoA desaturase (SREBP-SCD) axis (Zhang et al. 2017). In *C. elegans*, SBP-1 is the only homolog of sterol-regulatory element binding proteins (SREBPs). SREBPs are major regulators of lipid homeostasis, including fatty acids, triglycerides, and cholesterol in vertebrate cells (Goldstein *et al.* 2006; Shao and Espenshade 2012). Inactivation of SUR-7 restored the proper level of zinc and lowered fat accumulation and fatty acid profiles of *sbp-1(ep79)* via directly upregulating the activity of SCD (Zhang *et al.* 2017). Thus, this raised the question whether other zinc transport proteins were also involved in lipid metabolism. Therefore, we examined zinc transport related proteins in *C. elegans* and identified that the *cdf-1(n2527)* mutation acted as another suppressor of the *sbp-1(ep79)* mutant to restore its zinc levels and lipid content. This result provides further consistent evidence to link zinc homeostasis and lipid metabolism.

Materials and methods
Nematode strains, RNA interference, and culture conditions
C. elegans strains were maintained on NGM plates with Escherichia. coli *OP50* under standard culture conditions, unless otherwise specified. RNA interference (RNAi) was performed using the feeding method (Wu *et al.* 2018) and the bacterial strains feed were from the Ahringer *C. elegans* RNAi library. The wild-type strain was Bristol N2 (WT). All worm strains used in this study are listed in Supplementary Table S1.

Construct of *sur-7*RNAi clone
Construction of the *sur-7*RNAi used the *L4440* empty vector (EV). The PCR primers used for the amplified EV and *sur-7* gene are shown in Supplementary Table S2. These two linearized DNA fragments were recombined following the instruction of ClonExpress MultiS One Step Cloning Kit (Vazyme Biotech Co., Ltd), and then transformed into HT115 competent cells.

Construction of transgenic strains
Construction of the *WT; kunEx203[cdf-1p::cdf-1::gfp, myo-2p::mcherry]* and *WT; kunEx187[sur-7p::sur-7::gfp, rol-6(su1006)]* transgenic strains were done as follows. In general, DNA fragments of specific genes and their related promoters were isolated using PCR. The amplified DNA fragments were subsequently inserted into the transgenic plasmid *pPD95.75* (Frøkjær-Jensen *et al.* 2008). An injection mixture with 50 ng/μL transgenic plasmid and 5 ng/μL *pCFJ90(myo-2p::mcherry)* or *rol-6(su1006)* were injected into the gonads of young adult wild type N2 worms. The positive transgenic worms were selected based on fluorescence

expression. The primers for the construction of transgenic worms are listed in Supplementary Table S2.

Nile Red staining of fixed worms and quantification of lipid droplet size
Nile Red staining of fixed worms was performed as previously described (Brooks *et al.* 2009; Liang *et al.* 2010). Young adult worms were collected and suspended in 1 mL of water on ice, then resuspended in 1 mL of buffer M9 with 50 μL of freshly prepared 10% paraformaldehyde solution. Worms were frozen in liquid nitrogen, subjected to two or three incomplete freeze/thaw cycles, and then washed with M9 buffer several times to remove the paraformaldehyde solution. Two microliters of 5 mg/mL Nile Red was added to the worm pellet (1 mL) and incubated for 30 min at 20°C, with occasional gentle agitation. Worms were washed two or three times with M9 buffer and mounted onto 2% agarose pads for microscopic observation and photography. For each animal, a projection image with proper intensity was acquired using an Olympus BX53 fluorescence microscope (Japan) (Shi *et al.* 2013). At least 15 animals were imaged, and lipid droplet (LD) size was quantified from approximately five worms for each worm strain or treatment.

Analysis of fatty acid compositions
Approximately 2000 young adults were harvested for fatty acid esterification and analysis. The harvested worms' fatty acids were esterified with 1 mL of MeOH + 2.5% H_2SO_4 and heated for 1 hour at 70°C. Determination of the fatty acids was done using an Agilent 7890 series gas chromatographer equipped with a 15 m × 0.25 mm × 0.25 μm DB-WAX column (Agilent, Santa Clara, California, USA), with helium as the carrier gas at 1.4 mL/min, and a flame ionization detector. Four biological replicates were performed for gas chromatography (GC) analysis.

Analysis of triacylglycerol
About 4×10^4 synchronized young adults were harvested for total lipid extraction. Triacylglycerol (TAG) and phospholipids (PL) were separated by thin-layer chromatography, and the determination of fatty acids was by GC using an Agilent 7890A. The methyl ester of C15:0 was used as a standard for quantitative analysis.

Supplementation or sequestration of zinc
$ZnSO_4$ supplementation and zinc reduction by N, N, N′,N′-tetrakis (2-pyridylmethyl) ethylenediamine (TPEN) were performed as described previously (Zhang *et al.* 2017). In brief, synchronized L1 worms were placed and cultivated on NGM plates supplied with either $ZnSO_4$ or TPEN with a final concentration of 50 μM and 5 μM, respectively, and young adult worms were harvested for further analysis.

Zinpyr-1 staining and visualization
Zinpyr-1 staining was performed as described previously (Roh *et al.* 2013). The fluorescence of Zinpyr-1 was visualized under an OLYMPUS BX53 fluorescence microscope (Olympus). Images were captured using identical settings and exposure times, unless specifically noted. The fluorescence intensity was quantified using Photoshop software (Błażewicz *et al.* 2013).

Visualization of GFP
L4 and young adult GFP positive worms were picked and plated on an agarose gel pad and visualized using a two-photon confocal microscope (Nikon A1MP+) or a fluorescent microscope (BX53;

Olympus). Images were captured using the same settings and exposure times for each worm, unless specifically indicated, and the GFP reporter expression was quantified using Photoshop software.

Growth rate assay

The gravid adult worms were treated with alkaline hypochlorite and the eggs were obtained. These were then seeded onto NGM plates and cultured for several days until adulthood. Forty-eight hours after seeding, the number of adults and the total number of worms were scored under a microscope every 12 hours. Each strain underwent three biological replications.

Data analysis

Data are presented as the mean ± SEM, except when specifically indicated. Statistical analysis was conducted using Student's *t*-test. Figures were made using GraphPad Prism 6 (GraphPad Software, La Jolla, CA, USA) and Adobe Illustrator CS6.

Data availability

All data necessary for confirming the conclusions in this article are included in this article and in supplemental figures and tables. Worm strains or plasmids constructed by us are available upon request. Supplemental Material available at figshare: https://doi.org/10.25387/g3.14301467.

Results

The cation diffusion facilitator CDF-1 maintained zinc homeostasis and lipid metabolism

In eukaryotic cells, two major families of zinc transport proteins, cation diffusion facilitators [CDF/ZnT/SLC30] and zrt-, irt-like proteins (ZIP/SLC39)], mediate zinc trafficking and homeostasis. In total, 14 CDFs and 14 ZIPs in *C. elegans* have been identified with the homologous protein sequences to the 10 CDF and 14 ZIP proteins in *Homo sapiens* (Kambe *et al.* 2015) (Supplementary Figure S1). We previously reported on zinc transport protein SUR-7, which coordinately affects zinc homeostasis and lipid metabolism (Zhang *et al.* 2017). To explore whether the other related transporters are also involved in zinc homeostasis and lipid metabolism, we tested 11 of the 28 zinc-related transporters, that had available mutants, to detect their labile zinc and pseudocoelomic zinc by zinpyr-1 fluorescence and their LDs by Nile Red staining (Brooks *et al.* 2009; Roh *et al.* 2013).

Zinpyr-1 staining showed a differential intensity and location of fluorescence among the various worm mutants under treatment with or without $ZnSO_4$. (Figure 1, A and B, Supplementary Figure S2). Under normal conditions, like the *sur-7(tm6523)* mutant, the *cdf-1(n2527)*, *zipt-2.3(ok2094)*, and *zipt-15(ok2160)* mutants displayed reduced fluorescence (Figure 1, A and B, Supplementary Figure S2). This was mainly restricted in the area of the intestine lumen, suggesting a defect in zinc uptake. In contrast, the majority of mutants, especially the *ttm-1(tm6669)* mutant, displayed higher zinpyr-1 fluorescence than the wild type N2 (Figure 1, A and B, Supplementary Figure S2). In the presence of $ZnSO_4$, most mutants of the tested zinc-related transporters showed an increased level of Zinpyr-1 fluorescence to some extent (Figure 1, A and B, Supplementary Figure S2). Interestingly, among the 11 transporter mutants, only the *cdf-1(n2527)* mutant displayed a reduced LD size and lipid accumulation similar to the *sur-7(tm6523)* mutant in response to the $ZnSO_4$ treatment. However, the LD size and lipid accumulation of the other worms were not altered under normal conditions (Figure 1, C and D,

Supplementary Figure S3). Furthermore, consistent with our previous report (Zhang *et al.* 2017), reduction of zinc by TPEN [*N, N, N′, N′*-Tetrakis (2-pyridylmethyl) ethylenediamine], a zinc chelator, led to significantly increased LD size and lipid accumulation in all tested transporter mutants, like the wild type N2 (Figure 1, C and D, Supplementary Figure S3). Taken together, these results indicated that CDF-1 may function like SUR-7 in regulating zinc homeostasis and lipid metabolism.

Inactivation of CDF-1 reversed lipid metabolism defects of the *sbp-1(ep79)* mutant

Our previous study showed that SUR-7 functions *via* the SREBP and its target SCD to regulate lipid metabolism (Zhang *et al.* 2017). Inactivation of *sur-7* restores the LD size of the *sbp-1(ep79)* mutant by upregulating the activity of SCD. As mentioned above, the *cdf-1(n2527)* mutant displayed similar phenotypes like the *sur-7(tm6523)* mutation in responses to zinc; therefore, we wondered whether CDF-1 also affected lipid metabolism *via* the SREBP-SCD axis.

SUR-7, CDF-1, and CDF-2 proteins belong to the CDF family, and they possess six conservative transmembrane domains (Supplementary Figures S1 and S4). The *cdf-1(n2527)* mutation contains an SNP in the third transmembrane domain, leading to a premature termination (Supplementary Figure S4A). The *cdf-2(tm788)* mutation contains an 804 bp deletion and 68 bp insertion, which causes a frame shift mutation (Supplementary Figure S4B). The *sur-7(tm6523)* mutation contains a 564 bp deletion and 4 bp insertion, which causes early termination of translation (Supplementary Figure S4C). To verify whether *cdf-1* could be a suppressor of *sbp-1(ep79)*, we constructed the *sbp-1(ep79); cdf-1(n2527)* double mutant. *sbp-1(ep79); sur-7(tm6523)* was used as positive control, while *sbp-1(ep79); cdf-2(tm788)* was used as negative control. As we expected, the LD size and TAG content of both *sbp-1(ep79); cdf-1(n2527)* and *sbp-1(ep79); sur-7(tm6523)*, but not the *sbp-1(ep79); cdf-2(tm788)* mutant were significantly increased compared to the *sbp-1(ep79)* mutant (Figure 2, A–C). Similarly, the *sbp-1(ep79); cdf-1(n2527)* worms developed to adulthood about 24 hours earlier than the *sbp-1(ep79)* worms (Figure 2D). Taken together, these results demonstrated that the *cdf-1(n2527)* mutation was another suppressor of the *sbp-1(ep79)* mutant, in that it could restore the lipid accumulation and growth rate of the *sbp-1(ep79)* mutant.

The suppression of *sbp-1(ep79)* by *cdf-1(n2527)* was related to zinc level

As our previous study demonstrated, the *sbp-1(ep79)* mutant displays increased level of Zinpyr-1 fluorescence but reduced lipid accumulation, which can be reversed by *sur-7(tm6523)* (Zhang *et al.* 2017). Consistently, like the *sbp-1(ep79); sur-7(tm6523)* mutant, the zinc level indicated by Zinpyr-1 fluorescence in the *sbp-1(ep79); cdf-1(n2527)* mutant was significantly reduced compared with the *sbp-1(ep79)* worms, even under the treatment of $ZnSO_4$ (Figure 3, A and B), suggesting the upregulated zinc level of *sbp-1(ep79)* mutant depends on the activity of SUR-7 and CDF-1.

As we mentioned above and as reported in our previous work (Zhang *et al.* 2017), zinc negatively regulates lipid accumulation, and zinc reduction leads to increased lipid accumulation. Next, we asked whether the restoration of lipid accumulation of the *sbp-1(ep79)* mutant by *cdf-1(n2527)* was related to the zinc level. Nile Red staining of fixed worms showed that the LD sizes of both the *sbp-1(ep79); cdf-1(n2527)* and *sbp-1(ep79); sur-7(tm6523)* mutants were significantly reduced to the level of the *sbp-1(ep79)*
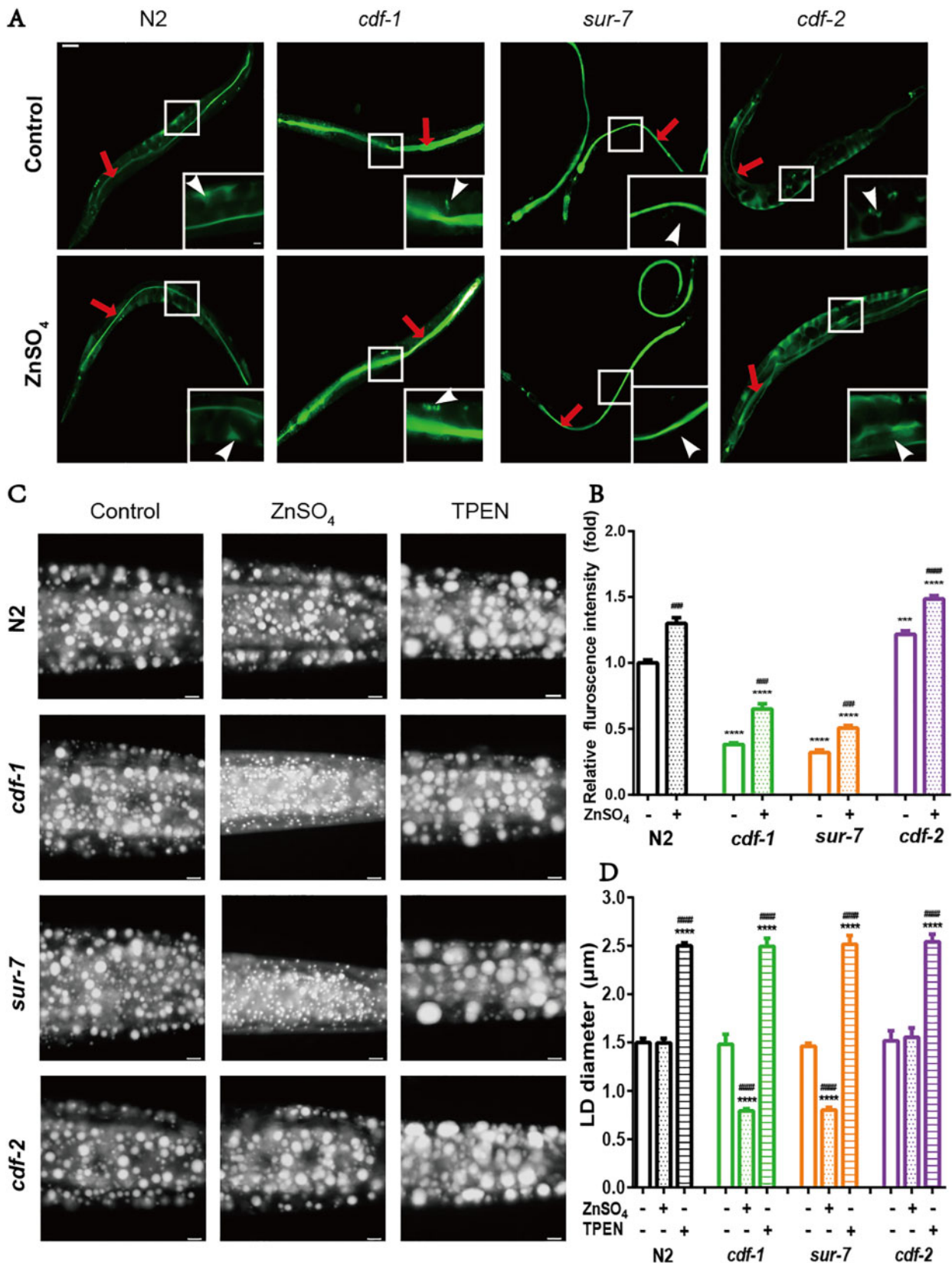
Figure 1 Zinc transporter mutants with zinc level and fat accumulation. (A) Fluorescence microscopy of WT, *cdf-1(n2527)*, *sur-7(tm6523)*, and *cdf-2(tm788)* treated with or without $ZnSO_4$, which stained with Zinpyr-1 and captured using identical settings and exposure times. Scale bar represents 50 μm for whole worms and 10 μm for enlarged worms. The concentration of $ZnSO_4$ is 50 μM. The red arrowheads indicate the lumen zinc and the white arrows show pseudocoelomic zinc. (B) Quantitation of the fluorescence intensity about pseudocoelomic zinc from (A). (C) Nile red staining of fixed worms treated with $ZnSO_4$ or TPEN. For representative animals, the anterior was on the left and the posterior was on the right; Bar, 5 μm. (D) Quantitation of lipid droplet size in the posterior region of intestines from five worms of each worm strain. The data are presented as mean ± SEM. For all statistical analysis, significant difference between WT N2 and a specific condition: ***$P < 0.001$; ****$P < 0.0001$ (unpaired *t*-test). Significant difference between the control and $ZnSO_4$/TPEN treatment of each strain: ###$P < 0.001$; ####$P < 0.0001$ (unpaired *t*-test).
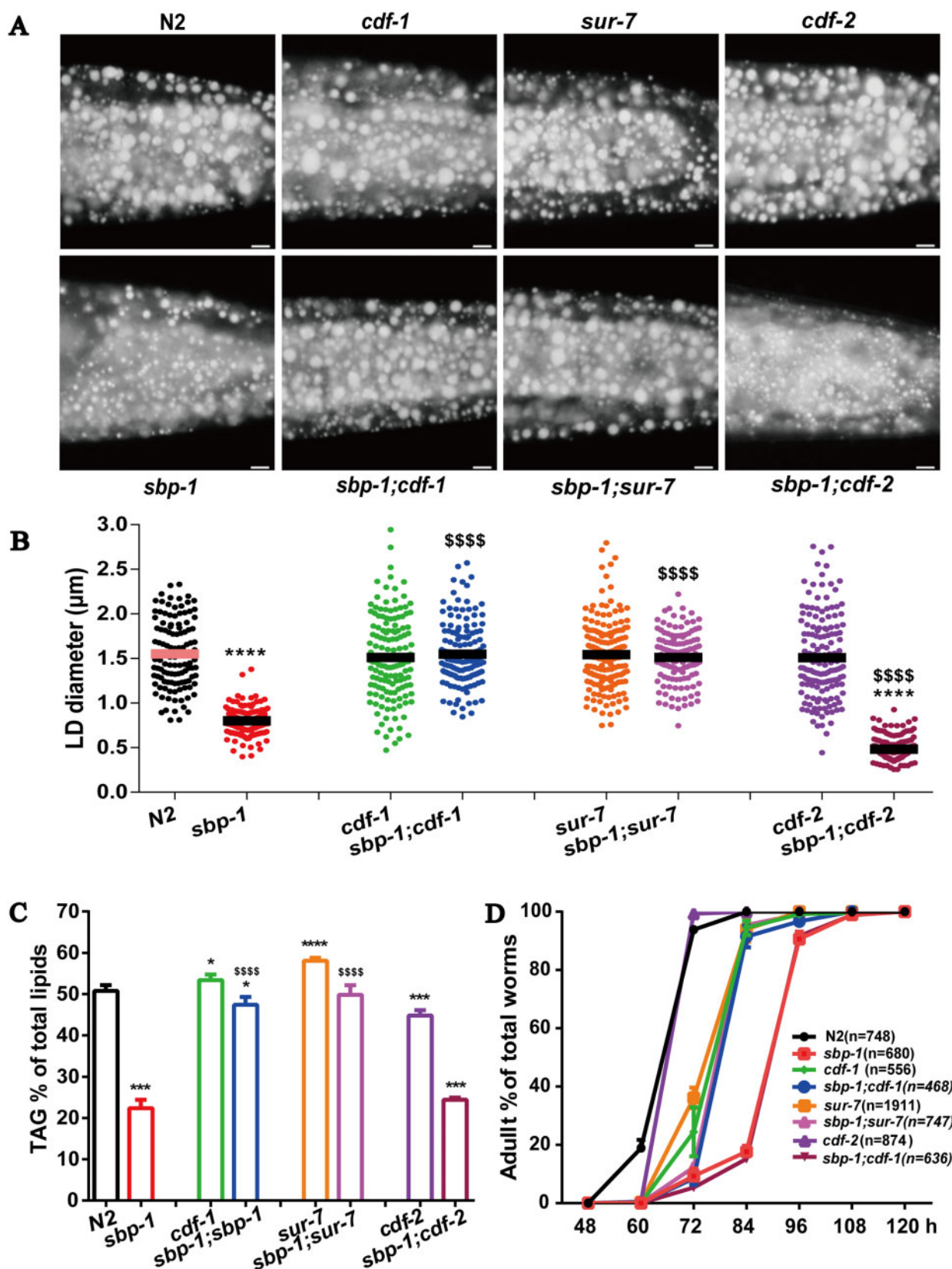
Figure 2 cdf-1 and *sur-7* restored lipid profiles of *sbp-1*. (A) The lipid droplets by Nile red staining in the worms of WT, *sbp-1(ep79)*, *cdf-1(n2527)*, *sbp-1(ep79; cdf-1(n2527))*, *sur-7(tm6523)*, *sbp-1(ep79); sur-7(tm6523)*, *cdf-2(tm788)*, and *sbp-1(ep79); cdf-2(tm788)*. For representative animals, the anterior was on the left and the posterior was on the right; Bar, 5 μm. (B) Quantitation of lipid droplet diameters in the posterior region of intestines from five worms of each worm strain. The data are presented as mean ± SEM. (C) The percentage content of triacylglycerol (TAG %) in total lipids (TAG+PL, phospholipids) of each worm strain. The data are presented as mean ± SEM of four biological repeats. (D) The growth rate of worms. The data are presented as the mean ± SEM with three biological repeats, *n*: the number of scored worms for each strain. For all statistical analysis, significant difference between WT N2 and each mutant: $^{*}P < 0.05$; $^{**}P < 0.01$; $^{***}P < 0.001$; $^{****}P < 0.0001$. Significant difference between *sbp-1(ep79)* and double mutant: $^{\$}P < 0.05$; $^{\$\$}P < 0.01$; $^{\$\$\$}P < 0.001$; $P < 0.0001$.
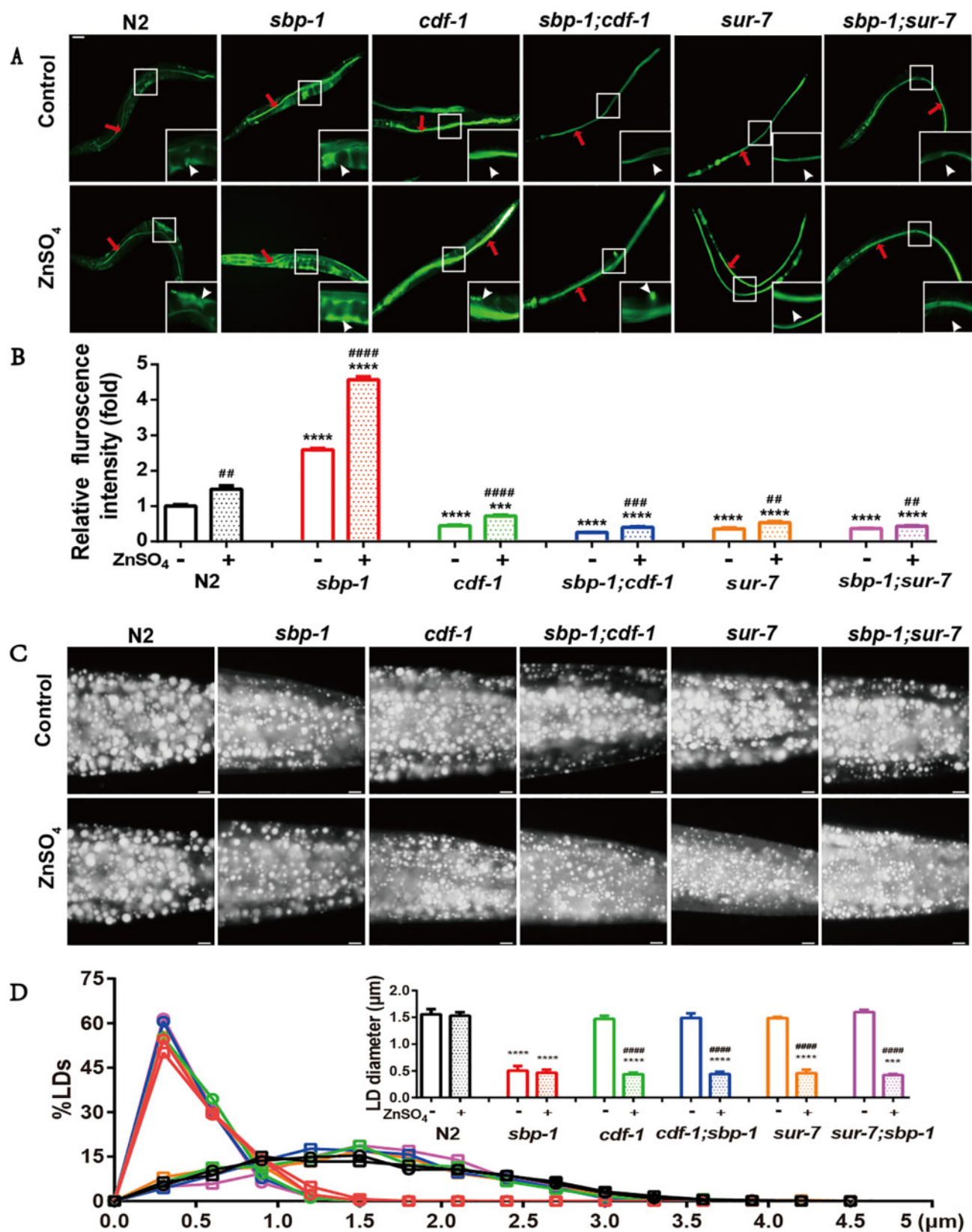
Figure 3 Zinc regulated fat accumulation in *C. elegans*. (A) zinc levels of WT, *sbp-1(ep79)*, *cdf-1(n2527)*, *sbp-1(ep79; cdf-1(n2527))*, *sur-7(tm6523)*, *sbp-1(ep79); sur-7(tm6523)*, *cdf-2(tm788)*, and *sbp-1(ep79); cdf-2(tm788)* treated with or without ZnSO₄ by stained with Zinpyr-1. Images were captured using identical settings and exposure times. Scale bar represents 50 μm for whole worms and 5 μm for enlarged worms. The concentration of ZnSO₄ is 50 μM. The red arrowheads indicate the lumen zinc accumulates of the intestine, and the white arrows show pseudocoelomic zinc. (B) Quantitation of the fluorescence intensity. (C) Nile red staining of fixed worms' lipid droplets; Bar, 5 μm. (D) Quantitation of lipid droplet size and frequency distribution of LD diameter in the posterior region of intestines from five worms of each worm strain. All of quantitation of the data is presented as mean ± SEM. For all statistical analysis, significant difference between N2 (WT) and a specific condition: $^*P < 0.05$; $^{**}P < 0.01$; $^{***}P < 0.001$; $^{****}P < 0.0001$. Significant difference between within groups of the control and ZnSO₄ treatment: $^{\#}P < 0.05$; $^{\#\#}P < 0.01$; $^{\#\#\#}P < 0.001$; $^{\#\#\#\#}P < 0.0001$ (unpaired *t*-test), which applies to all subsequent statistical analysis.

mutant when treated with ZnSO$_4$, similar to the *cdf-1(n2527)* or *sur-7(tm6523)* single mutant alone (Figure 3, C and D). However, the LD size in N2 and the *sbp-1(ep79)* mutant was not altered with the ZnSO$_4$ treatment (Figure 3, C and D). Taken altogether, these results further support a tight connection of lipid accumulation and zinc homeostasis regulated by SREBP-CDF-1/SUR-7.

CDF-1 regulated the activity of SCD

In *C. elegans*, FAT-5, FAT-6, and FAT-7 are three SCDs that convert the saturated fatty acids palmitic acid (C16:0) and stearic acid (C18:0) to palmitoleic acid [C16:1(n-7)] and oleic acid [C18:1(n-9)] (Brock *et al.* 2007; Shi *et al.* 2013; He *et al.* 2018). Our previous study showed that reduction of lipid accumulation in the *sur-7(tm6523)* mutant was due to a decreased conversion activity of SCD (Zhang et al. 2017). To confirm that the SCD conversion activity in the mutants involved *cdf-1(n2527)*, we detected their fatty acid profiles *via* GC under either TPEN or ZnSO$_4$ treatment. The levels of oleic acid C18:1(n-9) and the conversion activity of SCD [C18:1(n-9)/C18:0] were increased when treated with TPEN in all worm strains (Figure 4, A–C), while they were reduced in *cdf-1(n2527)* and *sur-7(tm6523)* mutants in the presence of ZnSO$_4$ (Figure 4, A–C). Meanwhile, the levels of saturated fatty acids (C16:0 and C18:0) in *sbp-1(ep79); cdf-1(n2527)* and *sbp-1(ep79); sur-7(tm6523)* mutants were reduced compared with the *sbp-1(ep79)* mutant (Figure 4, A and D). Consistently, the SCD conversion activity was increased in both *sbp-1(ep79); cdf-1(n2527)* and *sbp-1(ep79); sur-7(tm6523)* mutants (Figure 4, C and F). Collectively, these results indicated that the *cdf-1(n2527)* mutant was similar to the *sur-7(tm6523)* mutant in response to dietary ZnSO$_4$ or TPEN treatment in regulating SCD activity.

Zinc promotes SCD expression but reversely inhibits its conversion activity

Since the *n2527* mutation of *cdf-1* suppressed the SCD activity under ZnSO$_4$ treatment, we therefore questioned whether it was due to the altered expression of SCDs. To test the expression of SCDs, we opted to use *cdf-1*RNAi and *sur-7*RNAi for experimental convenience. Meanwhile, we constructed two transgenic strains, WT; *kunEx203[cdf-1p::cdf-1::gfp, myo-2p::mcherry]* and WT; *kunEx187[sur-7p::sur-7::gfp, rol-6(su1006)]*. The CDF-1::GFP is mainly expressed in the intestine and SUR-7::GFP is mainly expressed in the muscle. The *cdf-1*RNAi specifically inhibited the fluorescence expression of CDF-1::GFP but not SUR-7::GFP. Likewise, the *sur-7*RNAi only inhibited the fluorescence expression of SUR-7::GFP but not CDF-1::GFP, suggesting the efficiency and specification of each gene RNAi (Supplementary Figure S5). The fluorescence intensity of FAT-5::GFP, FAT-6::GFP, and FAT-7::GFP was not changed in the *cdf-1*RNAi and *sur-7*RNAi worms compared to the control (EV) (Figure 5). Interestingly, distinguished from the SCD conversion activity (Figure 4C), the fluorescence intensity of FAT-5::GFP, FAT-6::GFP, and FAT-7::GFP was significantly increased in the presence of ZnSO$_4$ but was decreased under zinc reduction by TPEN treatment in control (EV), *cdf-1*RNAi, and *sur-7*RNAi worms (Figure 5), which were contradictory with the SCD conversion activity reduced under ZnSO$_4$ or increased TPEN treatment. Nevertheless, these results suggest that zinc promotes SCD expression but reversely inhibits its conversion activity.

Discussion

Zinc is an essential element for living organisms. Dysfunction of zinc homeostasis is associated with lipid metabolism–related diseases. Our previous work uncovered a cation diffusion facilitator, SUR-7, that is required for the function of SREBP-SCD in lipid synthesis and accumulation in *C. elegans*. In this study, we further identified another cation diffusion facilitator, CDF-1, from among other zinc-related transporters that functions similarly to SUR-7 in regulating lipid metabolism. We propose a model (Figure 6) to better illustrate the function of CDF-1/SUR-7 in lipid metabolism. Under normal conditions, CDF-1/SUR-7 may be involved in zinc uptake and transportation for the maintenance of zinc homeostasis as well as the downregulation of fatty acid biosynthesis and lipid accumulation. Inactivation of CDF-1 or SUR-7 impairs zinc uptake and transportation, which results in the reduction of free zinc levels that consequently upregulate the conversion activity of SCD, further promoting the biosynthesis of unsaturated fatty acids and increasing lipid accumulation (Figure 6).

Zinc transport proteins play crucial roles in maintaining zinc homeostasis. Dysfunction of ZnTs is associated with obesity and diabetes (Quraishi *et al.* 2005; Noh *et al.* 2014; Morais *et al.* 2019). In *C. elegans*, a total of 28 potential zinc transport proteins have been identified based on human protein sequence homologues (Kambe *et al.* 2015). Among these zinc transport proteins, we found that CDF-1 and SUR-7 function redundantly to regulate zinc homeostasis and lipid metabolism. Inactivation of either CDF-1 or SUR-7 reduced Zinpyr-1 fluorescence in wild-type N2 and also in the *sbp-1(ep79)* mutant. More importantly, both gene mutations could recover the LD size in the *sbp-1(ep79)* mutant, and both displayed a similar response with a reduction of LD size under ZnSO$_4$ treatment. Therefore, our current work in *C. elegans* also supports a negative relationship between zinc level and lipid accumulation.

In this study, some transporter mutants showed higher levels of zinc than wild type, and some showed lower levels of zinc than wild type, but not all of them could rescue *sbp-1*. This could be due to different, specific expression locations of these ZnTs, and because the routes of zinc transport in various cell types may be different as well (Kambe *et al.* 2015). Another reason can be based on a different structure-function of these ZnTs (Cotrim *et al.* 2019). Moreover, the expressions of different ZnTs at different stages of disease may be altered. For example, the expression level of specific ZnTs identified in the whole blood of patients with systemic inflammatory response syndrome at admission and on day 7 of ICU was different (Florea *et al.* 2018). By previous reports, some transporter mutants are very sensitive to zinc. The other ZnTs could not transport excessive zinc from the pseudo-coelome (Yoder *et al.* 2004; Davis *et al.* 2009), resulting in high levels of zinc in the pseudocoelome. Therefore, it is possible that not all of these zinc transport mutants are sensitive to zinc and thus affect fat synthesis. At this time, only two mutants, *cdf-1* and *sur-7*, have been found to be extremely sensitive to zinc, affecting fat synthesis through zinc level (Figure 1). While the zinc content is lower in *zipt-2.3* and *zipt-15* mutants under normal conditions (Supplementary Figure S2), which is consistent with the *cdf-1* and *sur-7* mutants, however the zinc content in the pseudocoelome is significantly increased when zinc is supplemented. The response of the *zipt-2.3* and *zipt-15* mutants to an excess of zinc is clearly different from the *cdf-1* and *sur-7* mutants. This may be one of the reasons why the zinc content of *zipt-2.3* and *zipt-15* mutants is reduced under normal conditions but could not restore the phenotype(s) of *sbp-1(ep79)*. In addition, different subunits of the same protein can have different locations and functions. Through expression from different transcriptional start sites, *C. elegans* TTM-1 encodes two proteins TTM-1A and TTM-1B. TTM-1A is localized to vesicles and may also promote zinc
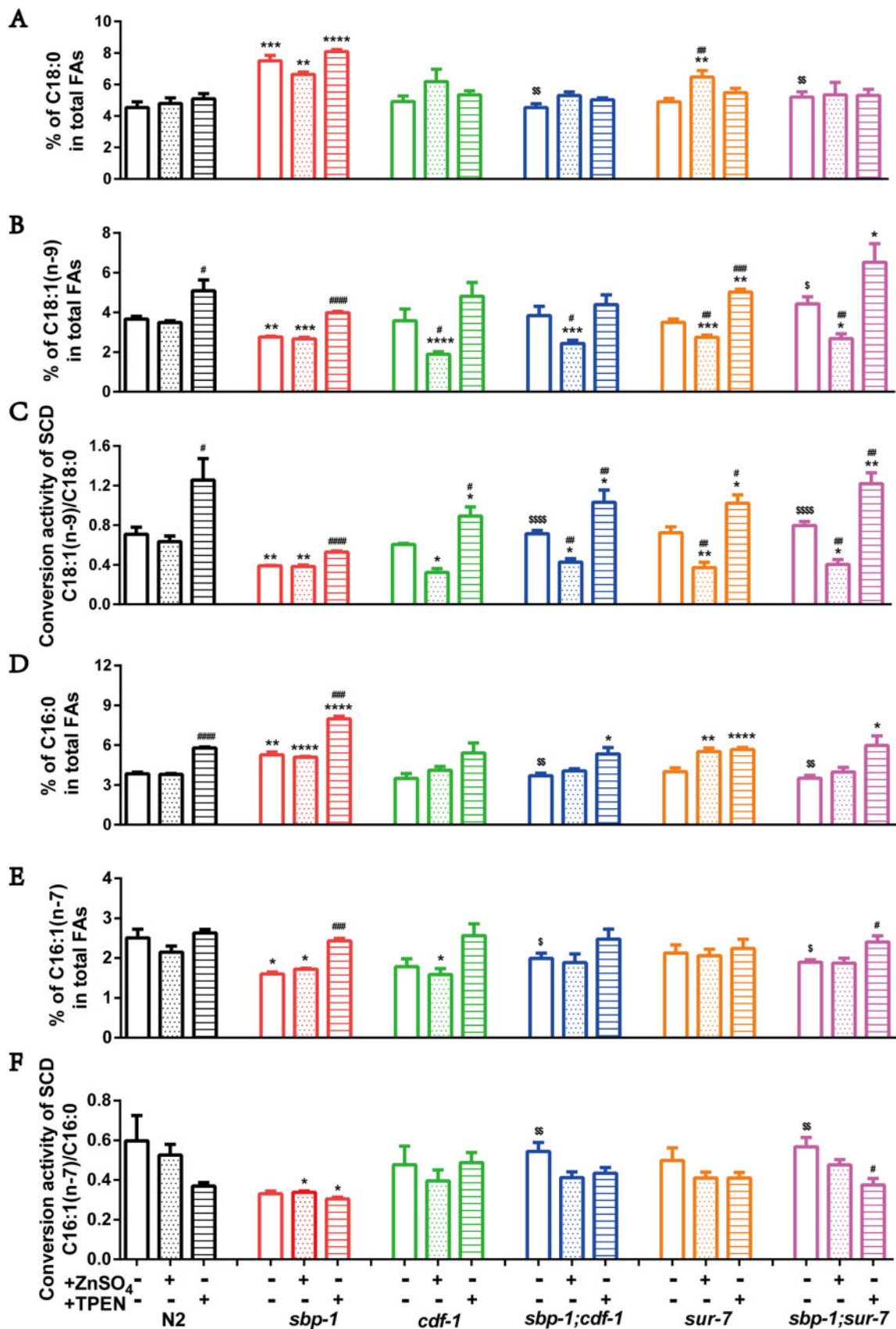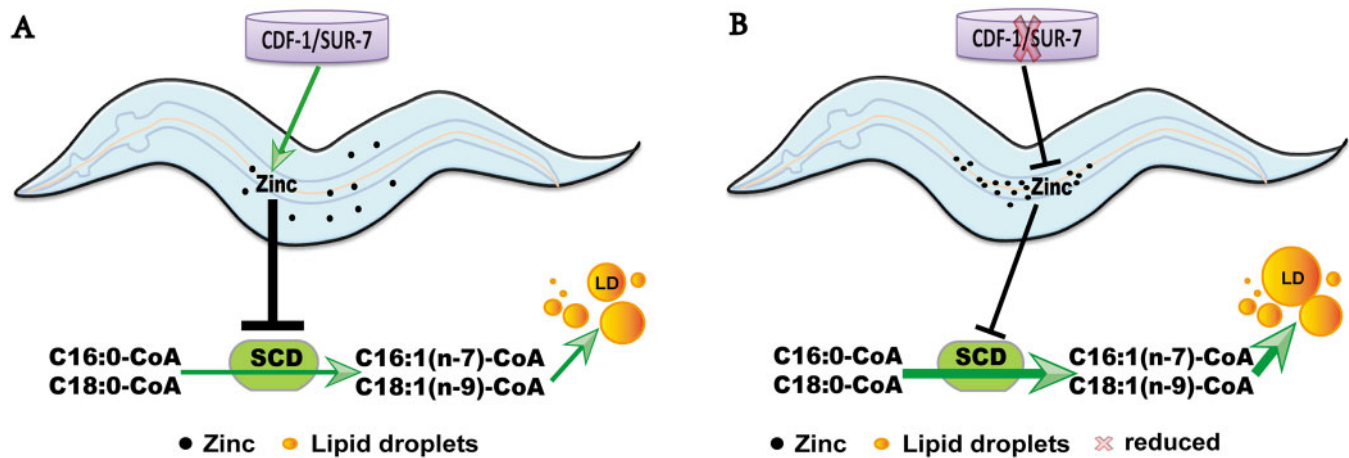
Figure 4 cdf-1 and *sur-7* mediated the activity of SCD by zinc. (A), (B), (D), and (E) The fatty acid profiles of N2 (WT), *sbp-1(ep79)*, *cdf-1(n2527)*, *sbp-1(ep79; cdf-1(n2527))*, *sur-7(tm6523)* and *sbp-1(ep79); sur-7(tm6523)* were quantified using GC analysis. (A) and (B) Percentage of C18:0 and C18:1(n-9) in total fatty acids. (C) The conversion activity of SCD presented by the ratio of C18:1(n-9)/C18:0. (D) and (E) Percentage of C16:0 and C16:1(n-7) in total fatty acids. (F) The conversion activity of SCD presented by the ratio of C16:1(n-7)/C16:0. The data are presented as mean ± SEM of more than three biologic repeats.
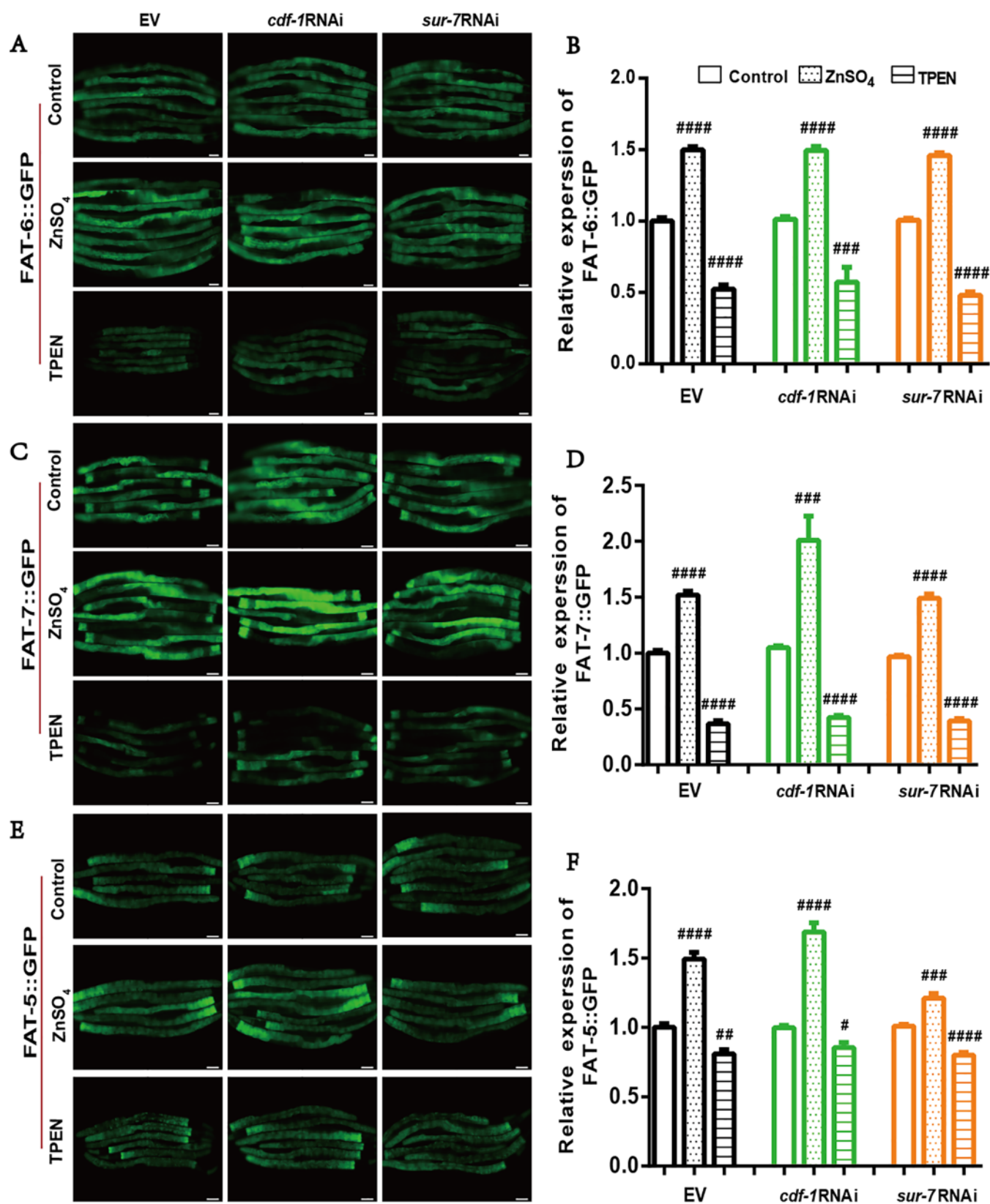
Figure 5 The expression of FAT-6::GFP, FAT-7::GFP, and FAT-5::GFP under empty vector or a specific condition. (A), (C), and (E) The fluorescence intensity of FAT-6::GFP, FAT-7::GFP, and FAT-5::GFP. Bar, 50 μm. From left to right were EV, *cdf-1*RNAi, and *sur-7*RNAi, from top to bottom were control, $ZnSO_4$ supplementation, and TPEN supplementation. (B), (D), and (F) The quantization of the GFP fluorescence intensity corresponding to figure (A), (C), (E), respectively.

Figure 6 A working model of how CDF-1 and SUR-7 mediate zinc to regulate SCD activity in lipid metabolism. (A) Under normal condition, CDF-1 and SUR-7 promote the transport of zinc into the worm body, which prevented SCD from over activation to maintain the biosynthesis of MUFAs and fat accumulation. (B) As CDF-1 and SUR-7 were impaired, zinc transporting into the worm body from the lumen was blocked, which enhanced the activity of SCD thus promoting the biosynthesis of MUFAs and accelerating fat accumulation.

excretion and/or sequestration, TTM-1B functions in excretion; it is localized to the apical surface of the plasma membrane of intestinal cells and transports cytoplasmic zinc into the intestinal lumen (Roh *et al.* 2013). Therefore, it is understandable that other ZnTs could not restore the phenotypes in a SBP-1 mutant.

While CDF-1 and SUR-7 depletion have a similar effect on the zinc and lipid levels of *sbp-1(ep79)* worms, Zinpyr-1 stained *cdf-1(n2527)* and *sur-7(tm6523)* worms look different. *cdf-1* worms show stronger luminal Zinpyr-1 staining than *sur-7* worms (Figures 1A and 3A). The *sur-7* mutant was more tolerant to high Zn^{2+} concentrations than *cdf-1* mutant (Yoder *et al.* 2004). These differences between *cdf-1* and *sur-7* may be related to their different subcellular localization and reflect functional differences. Moreover, in *C. elegans*, SUR-7, located in the ER membrane (Supplementary Figure S5C) (Yoder *et al.* 2004), may transport zinc from the cytoplasm into the ER. CDF-1 promotes zinc excretion into the pseudocoelomic space (Supplementary Figure S5A) (Bruinsma *et al.* 2002; Davis *et al.* 2009). CDF-2 transports excess zinc into lysosome-related vesicles (Davis *et al.* 2009). TTM-1A is distributed in a punctate pattern in intestinal and hypodermal cells and promotes zinc excretion and/or sequestration, while TTM-1B transports zinc into the intestinal lumen (Roh *et al.* 2013). We analyzed mRNA levels of these genes using quantitative real-time PCR (qPCR) in the *cdf-1* or *sur-7* mutant (Supplementary Figure S6, A– C). The expression of *ttm-1a* increased in the *sur-7* mutant and the level of *ttm-1b* was higher in the *cdf-1* mutant (Supplementary Figure S6, A and B). This result suggested that the function of TTM-1B in *cdf-1* worms was enhanced which accelerated zinc to the intestinal lumen, while the function of TTM-1A in *sur-7* worms was enhanced which promoted zinc to the punctate organelles. Therefore, we suggest that the capacity of zinc is different between the organelles or organs in *C. elegans*, which leads to the different sensitivity of mutants to zinc and the different response of mutants in lipid metabolism.

SCD is a main target of SREBP. SCD converts saturated fatty acids (C16:0 and C18:0) to Monounsaturated fatty acids (MUFAs) [C16:1(n-7) and C18:1(n-9)] for the biosynthesis of TAGs, PLs, and cholesterol esters. The SCD catalysis is dependent on its di-iron center. We previously showed that zinc reduction led to iron overload, consequently activating the conversion activity of SCD and fat accumulation (Zhang *et al.* 2017). Although the expression

of FAT-5::GFP, FAT-6::GFP, and FAT-7::GFP, the three SCDs in *C. elegans*, was upregulated by $ZnSO_4$ treatment while being downregulated by TPEN, the levels of oleic acid C18:1(n-9) and the conversion activity of SCD [C18:1(n-9)/C18:0] were increased under TPEN treatment. However, these were reduced in the *cdf-1(n2527)* and *sur-7(tm6523)* mutants by $ZnSO_4$ treatment. Thus, these results demonstrate a negative regulation of SCD expression and conversion activity by zinc, further confirming our hypothesis that zinc acts by bypassing SREBP to directly determine the conversion activity of SCD in lipid biosynthesis and accumulation. On the other hand, our results also showed that the expression of FAT-5::GFP, FAT-6::GFP, and FAT-7::GFP was upregulated upon $ZnSO_4$ feeding when CDF-1 and SUR-7 were depleted, but the conversion activity of SCD was decreased.

Upon the loss of function of SCDs, the phenotypes of the worms were very similar to *sbp-1(ep79)* worms, such as small LDs, which appeared very meager. So, does the loss of SCDs function also increase the zinc level like the loss of SBP-1 function? Is it possible to restore the phenotypes of SCDs loss of function with SUR-7 or CDF-1 depletion as well? Our results showed it partially did. *fat-6*RNAi worms had an increased level of zinc, and under either SUR-7 or CDF-1 depletion, the high zinc level in *fat-6*RNAi worms was rescued (Supplementary Figure S7, A and B). However, although *cdf-1* or *sur-7* mutants could restore the zinc level of *fat-6*RNAi worms, they could not restore the *fat-6*RNAi lipid droplets back to wild type. They still look meager (Supplementary Figures S7, C and D). This observation raises the question of whether the increased expression of SCDs might be due to feedback regulation by decreased levels of C18:1(n-9). Therefore, we speculate that targeting of SCD may potentially provide a possible treatment for zinc-related lipid metabolic diseases. This specific mechanism requires further study, however.

contributed reagents/materials/analysis tools. All authors reviewed the manuscript.

Funding

Conflicts of interest: The authors declare that they have no conflict of interest.

Literature cited

Baltaci AK, Yuce K. 2018. Zinc transporter proteins. Neurochem Res. 43:517–530.

Błażewicz A, Klatka M, Astel A, Partyka M, Kocjan R. 2013. Differences in trace metal concentrations (Co, Cu, Fe, Mn, Zn, Cd, And Ni) in whole blood, plasma, and urine of obese and nonobese children. Biol Trace Elem Res. 155:190–200.

Brock TJJ, Browse J, Watts JL. 2007. Fatty acid desaturation and the regulation of adiposity in *Caenorhabditis elegans*. Genetics. 176:865–875.

Brooks KK, Liang B, Watts JL 2009. The influence of bacterial diet on fat storage in C. elegans. PLoS One. 4:e7545.

Bruinsma JJ, Jirakulaporn T, Muslin AJ, Kornfeld K. 2002. Zinc ions and cation diffusion facilitator proteins regulate Ras-mediated signaling. Dev Cell. 2:567–578.

Chasapis CT, Loutsidou AC, Spiliopoulou CA, Stefanidou ME. 2012. Zinc and human health: an update. Arch Toxicol. 86:521–534.

Costarelli L, Muti E, Malavolta M, Cipriano C, Giacconi R, *et al.* 2010. Distinctive modulation of inflammatory and metabolic parameters in relation to zinc nutritional status in adult overweight/obese subjects. J Nutr Biochem. 21:432–437.

Cotrim CA, Jarrott RJ, Martin JL, Drew D. 2019. A structural overview of the zinc transporters in the cation diffusion facilitator family. Acta Crystallogr D Struct Biol. 75:357–367.

Cruz KJ, Morais JB, de Oliveira AR, Severo JS, Marreiro DD. 2017. The Effect of zinc supplementation on insulin resistance in obese subjects: a systematic review. Biol Trace Elem Res. 176:239–243.

Cuadrado A, Manda G, Hassan A, Alcaraz MJ, Barbas C, *et al.* 2018. Transcription factor NRF2 as a therapeutic target for chronic diseases: a systems medicine approach. Pharmacol Rev. 70:348–383.

Davis DE, Roh HC, Deshmukh K, Bruinsma JJ, Schneider DL, *et al.* 2009. The cation diffusion facilitator gene cdf-2 mediates zinc metabolism in *Caenorhabditis elegans*. Genetics. 182:1015–1033.

de Luis D, Pacheco AD, Izaola O, Terroba MC, Cuellar L, *et al.* 2013. Micronutrient status in morbidly obese women before bariatric surgery. Surg Obes Relat Dis. 9:323–327.

Drake I, Hindy G, Ericson U, Orho-Melander M. 2017. A prospective study of dietary and supplemental zinc intake and risk of type 2 diabetes depending on genetic variation in SLC30A8. Genes Nutr. 12:30.

Ennes Dourado Ferro F, de Sousa Lima VB, Mello Soares NR, Franciscato Cozzolino SM, do Nascimento Marreiro D. 2011. Biomarkers of metabolic syndrome and its relationship with the zinc nutritional status in obese women. Nutr Hosp. 26:650–654.

Escobedo-Monge MF, Ayala-Macedo G, Sakihara G, Peralta S, Almaraz-Gomez A, *et al.* 2019. Effects of zinc supplementation on nutritional status in children with chronic kidney disease: a randomized trial. Nutrients. 11:2671.

Florea D, Molina-Lopez J, Hogstrand C, Lengyel I, de la Cruz AP, *et al.* 2018. Changes in zinc status and zinc transporters expression in whole blood of patients with Systemic Inflammatory Response Syndrome (SIRS). J Trace Elem Med Biol. 49:202–209.

Frøkjær-Jensen C, Wayne Davis M, Hopkins CE, Newman BJ, Thummel JM, *et al.* 2008. Single-copy insertion of transgenes in *Caenorhabditis elegans*. Nat Genet. 40:1375–1383.

Fukada T, Yamasaki S, Nishida K, Murakami M, Hirano T. 2011. Zinc homeostasis and signaling in health and diseases: zinc signaling. J Biol Inorg Chem. 16:1123–1134.

Fukunaka A, Fujitani Y. 2018. Role of zinc homeostasis in the pathogenesis of diabetes and obesity. Int J Mol Sci. 19:476.

Goldstein JL, DeBose-Boyd RA, Brown MS. 2006. Protein sensors for membrane sterols. Cell. 124:35–46.

He B, Zhang J, Wang Y, Li Y, Zou X, *et al.* 2018. Identification of cytochrome b5 CYTB-5.1 and CYTB-5.2 in *C. elegans*; evidence for differential regulation of SCD. Biochim Biophys Acta Mol Cell Biol Lipids. 1863:235–246.

Kambe T, Tsuji T, Hashimoto A, Itsumura N. 2015. The physiological, biochemical, and molecular roles of zinc transporters in zinc homeostasis and metabolism. Physiol Rev. 95:749–784.

Kimura T, Kambe T. 2016. The functions of metallothionein and ZIP and ZnT transporters: an overview and perspective. Int J Mol Sci. 336.17:

Liang B, Ferguson K, Kadyk L, Watts JL. 2010. The role of nuclear receptor NHR-64 in fat storage regulation in *Caenorhabditis elegans*. PLoS One. 5:e9869.

Liu MJ, Bao S, Bolin ER, Burris DL, Xu X, *et al.* 2013. Zinc deficiency augments leptin production and exacerbates macrophage infiltration into adipose tissue in mice fed a high-fat diet. J Nutr. 143:1036–1045.

Liuzzi JP, Cousins RJ. 2004. Mammalian zinc transporters. Annu Rev Nutr. 24:151–172.

Miao X, Sun W, Fu Y, Miao L, Cai L. 2013. Zinc homeostasis in the metabolic syndrome and diabetes. Front Med. 7:31–52.

Morais JBS, Severo JS, Beserra JB, de Oiveira ARS, Cruz KJC, *et al.* 2019. Association between cortisol, insulin resistance and zinc in obesity: a mini-review. Biol Trace Elem Res. 191:323–330.

Noh H, Paik HY, Kim J, Chung J. 2014. The changes of zinc transporter ZnT gene expression in response to zinc supplementation in obese women. Biol Trace Elem Res. 162:38–45.

Olechnowicz J, Tinkov A, Skalny A, Suliburska J. 2018. Zinc status is associated with inflammation, oxidative stress, lipid, and glucose metabolism. J Physiol Sci. 68:19–31.

Quraishi I, Collins S, Pestaner JP, Harris T, Bagasra O. 2005. Role of zinc and zinc transporters in the molecular pathogenesis of diabetes mellitus. Med Hypotheses. 65:887–892.

Roh HC, Collier S, Deshmukh K, Guthrie J, Robertson JD, *et al.* 2013. ttm-1 encodes CDF transporters that excrete zinc from intestinal cells of *C. elegans* and act in a parallel negative feedback circuit that promotes homeostasis. PLoS Genet. 9:e1003522.

Rutter GA, Chimienti F. 2015. SLC30A8 mutations in type 2 diabetes. Diabetologia. 58:31–36.

Shao W, Espenshade PJ. 2012. Expanding roles for SREBP in metabolism. Cell Metabol. 16:414–419.

Shi X, Li J, Zou X, Greggain J, R⊘Dkær SV, *et al.* 2013. Regulation of lipid droplet size and phospholipid composition by stearoyl-CoA desaturase. J Lipid Res. 54:2504–2514.

Thokala S, Bodiga VL, Kudle MR, Bodiga S. 2019. Comparative response of cardiomyocyte ZIPs and ZnTs to extracellular zinc and TPEN. Biol Trace Elem Res. 192:297–307.

Virgili F, Ambra R, McCormack J, Simpson EEA, Ciarapica D, *et al.* 2018. Genetic polymorphisms and zinc status: implications for supplementation in metabolic diseases. Curr Pharm Des. 24: 4131–4143.

Wang S, Luo M, Zhang Z, Gu J, Chen J, *et al.* 2016. Zinc deficiency exacerbates while zinc supplement attenuates cardiac hypertrophy in high-fat diet-induced obese mice through modulating p38 MAPK-dependent signaling. Toxicol Lett. 258:134–146.

Wenzlau JM, Hutton JC. 2013. Novel diabetes autoantibodies and prediction of type 1 diabetes. Curr Diab Rep. 13:608–615.

Wu J, Jiang X, Li Y, Zhu T, Zhang J, *et al.* 2018. PHA-4/FoxA senses nucleolar stress to regulate lipid accumulation in *Caenorhabditis elegans*. Nat Commun. 9:1195.

Xu K, Zha M, Wu X, Yu Z, Yu R, *et al.* 2011. Association between rs13266634 C/T polymorphisms of solute carrier family 30 member 8 (SLC30A8) and type 2 diabetes, impaired glucose tolerance, type 1 diabetes–a meta-analysis. Diabetes Res Clin Pract. 91: 195–202.

Yoder JH, Chong H, Guan KL, Han M. 2004. Modulation of KSR activity in *Caenorhabditis elegans* by Zn ions, PAR-1 kinase and PP2A phosphatase. EMBO J. 23:111–119.

Zhang JJ, Hao JJ, Zhang YR, Wang YL, Li MY, *et al.* 2017. Zinc mediates the SREBP-SCD axis to regulate lipid metabolism in *Caenorhabditis elegans*. J Lipid Res. 58:1845–1854.

Communicating editor: S. Lee